^{40}Ti β decay and the neutrino capture cross section of ^{40}Ar

W. Trinder, R. Anne, M. Lewitowicz, M.G. Saint-Laurent, C. Donzaud, D. Guillemaud-Mueller, S. Leenardt, a C. Mueller, F. Pougheon, O. Sorlin, et al.

▶ **To cite this version:**

W. Trinder, R. Anne, M. Lewitowicz, M.G. Saint-Laurent, C. Donzaud, et al.. ^{40}Ti β decay and the neutrino capture cross section of ^{40}Ar. Physics Letters B, 1997, 415, pp.211-216. 10.1016/S0370-2693(97)01243-4 . in2p3-00014323

HAL Id: in2p3-00014323
https://hal.in2p3.fr/in2p3-00014323

Submitted on 21 Dec 1998

HAL is a multi-disciplinary open access archive for the deposit and dissemination of scientific research documents, whether they are published or not. The documents may come from teaching and research institutions in France or abroad, or from public or private research centers.

L'archive ouverte pluridisciplinaire **HAL**, est destinée au dépôt et à la diffusion de documents scientifiques de niveau recherche, publiés ou non, émanant des établissements d'enseignement et de recherche français ou étrangers, des laboratoires publics ou privés.

GANIL

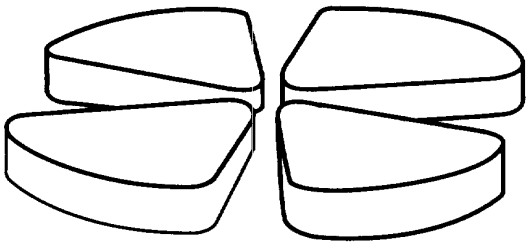

CERN LIBRARIES, GENEVA
SCAN-9708008

^{40}Ti β decay and the Neutrino Capture Cross Section of ^{40}Ar

W. Trinder[a)], R. Anne[a)], M. Lewitowicz[a)], M.G. Saint-Laurent[a)], C. Donzaud[b)], D. Guillemaud-Mueller[b)], S. Leenardt[b)], A.C. Mueller[b)], F. Pougheon[b)], O. Sorlin[b)], M. Bhattacharya[c)], A. García[c)], N.I. Kaloskamis[c)], E.G. Adelberger[d)], H.E. Swanson[d)]

[a)] *GANIL, B.P. 5027, 14076 Caen Cedex 5, France,*

[b)] *Institut de Physique Nucléaire, CNRS-IN2P3, 91406 Orsay Cedex, France,*

[c)] *University of Notre Dame, Notre Dame, IN 46556, USA,*

[d)] *University of Washington, Seattle, WA 98195, USA*

GANIL P 97 24

^{40}Ti β decay and the Neutrino Capture Cross Section of ^{40}Ar

W. Trinder[a)], R. Anne[a)], M. Lewitowicz[a)], M.G. Saint-Laurent[a)], C. Donzaud[b)], D. Guillemaud-Mueller[b)], S. Leenardt[b)], A.C. Mueller[b)], F. Pougheon[b)], O. Sorlin[b)], M. Bhattacharya[c)], A. García[c)], N.I. Kaloskamis[c)], E.G. Adelberger[d)], H.E. Swanson[d)]

[a)] *GANIL, B.P. 5027, 14076 Caen Cedex 5, France,*

[b)] *Institut de Physique Nucléaire, CNRS-IN2P3, 91406 Orsay Cedex, France,*

[c)] *University of Notre Dame, Notre Dame, IN 46556, USA,*

[d)] *University of Washington, Seattle, WA 98195, USA*

Abstract: ^{40}Ti β decay was studied at GANIL using the LISE3 spectrometer. A decay scheme was deduced from twenty-one observed β-delayed proton transitions feeding the ground and first excited states of ^{39}Ca. The ^{40}Ti half-life was found to be 51.7(6) ms. These results imply that the ICARUS ^{40}Ar detector has an effective absorption cross section for ^{8}B solar neutrinos of $14.5(4)\times10^{-43}$ cm^2; 73% of the total cross section arises from Gamow-Teller transitions that were neglected in early estimates of the ICARUS efficiency.

The ICARUS large-volume liquid-argon time-projection chamber [1, 2] could provide useful information on the solar neutrino puzzle because it will detect neutrinos via $e^-(\nu_x,\nu_x)e^-$ scattering as well as via the ^{40}Ar(ν_e,e^-)^{40}K neutrino capture reaction. Information about possible neutrino-flavour oscillations can be drawn from the *ratio* of scattering and absorption events, but definitive conclusions about neutrino properties are possible only if the detection efficiencies for the neutral and charged-current processes are well known. The cross sections for $e^- + \nu_x$ scattering as well as for the Fermi neutrino capture can be calculated accurately [3, 2]. However, the Gamow-Teller capture cross sections depend on model-dependent nuclear matrix elements. A recent shell-model calculation predicted that Gamow-Teller transitions contribute about 67% to the total ^{40}Ar neutrino-capture cross section of ^{8}B neutrinos [2] so that an empirical determination of the Gamow-Teller cross section is necessary for a reliable analysis of the ICARUS solar neutrino signals.

The transition strengths, $B(GT)$, for the Gamow-Teller absorption reactions in ^{40}Ar can be deduced from the mirror β decays of ^{40}Ti. Under the assumption of isospin symmetry, the $B(GT)$ value for a ^{40}Ar neutrino capture transition to an excited state of ^{40}K is identical to the $B(GT)$ of the corresponding ^{40}Ti β decay to the mirror state of ^{40}Sc. The large energy release in ^{40}Ti decay assures that it can feed all states relevant for the Gamow-Teller contribution to the ICARUS signal. The single previous study of ^{40}Ti decay [4] demonstrated that Gamow-Teller transitions play an important role in the ^{40}Ar neutrino capture cross section, but statistical and systematic errors were not good enough to calibrate the ICARUS efficiency.

This letter describes a detailed study of the β-delayed proton emission of ^{40}Ti to the ground and first excited states of ^{39}Ca using the LISE3 spectrometer at GANIL [5]-[7]. A ^{40}Ti secondary beam of about 0.3 atoms/s was produced by bombarding a 300 μm ^{nat}Ni target with 82.6 A$\times$MeV ^{50}Cr ions. The secondary beam purity was enhanced by a 215 μm ^{9}Be degrader foil at the intermediate focal point and by the Wien velocity filter at the exit of LISE3. The ^{40}Ti activity was implanted into a 500 μm silicon detector (implantation detector), which was

positioned between two similar silicon counters for registering β rays (β detectors). Two additional 300 μm silicon detectors, one of which was position sensitive, were mounted upstream; these provided energy-loss and time-of-flight for identifying the isotopes transmitted through the LISE3 spectrometer. Five large-volume (70%) germanium detectors mounted close to the silicon detector array registered γ rays.

A total of 6.3×10^4 ^{40}Ti atoms was collected in two different implantation modes of about equal statistics. In the first setting, the ^{40}Ti implantation profile (FWHM $\approx$ 50 μm) was centered a depth of about 100 μm and thus nearer to the upstream β detector. In the second setting, the profile was shifted to the center of the implantation detector by replacing one of the 300 μm detectors into a 150 μm one. In the following, we denote these modes as setting 1 and setting 2, respectively.

The secondary beam contained contaminating proton emitters (0.3 ^{41}Ti atoms/s and 0.04 ^{37}Ca atoms/s) along with a strong contribution of the β-emitter ^{38}Ca (0.7 atoms/s). Therefore, in analysing the proton spectrum we included only those ^{40}Ti events that were separated from preceeding ^{41}Ti or ^{37}Ca implantations by five respective half-lives *and* whose decay events occured before the arrival of the next ^{40}Ti, ^{41}Ti or ^{37}Ca atom. The proton-energy scale was calibrated by comparing our ^{41}Ti proton lines to those observed in a recent high-resolution study of ^{41}Ti β decay [8]. Corrections were made for the slightly different implantation depths of ^{40}Ti and ^{41}Ti ions ($\Delta \approx 20$ μm), and for the non-linear recoil defect [9]. The detection efficiency for high-energy protons was obtained from a Monte-Carlo simulation based on the measured implantation depth profile.

Figure 1a shows the raw proton spectrum of setting 2 and Fig. 1b the proton spectrum of setting 1 under the condition of a small energy loss of the coincident β rays in the upstream β detector ($\Delta E_\beta \leq 650$ keV). The resolution in the raw spectrum is poor because the continously distributed energy-loss of the coincident β ray was added to each proton signal. Spectrum 1b has much better resolution because its condition selects for events where the β rays leave little energy in the implantation detector (for more details about this technique see [10, 11]). In addition to the strong proton lines at 1.322, 1.698, 2.159 and 3.733 MeV that are

visible in both spectra, several weak lines were identified only in spectrum 1b. A small contamination of ^{41}Ti protons is indicated by the peak (marked with a star in spectrum b) from the proton decay of the ^{41}Sc isobaric analog state (IAS). Its intensity could be determined by varying the above mentioned selection conditions. Two weak low-energy proton lines were identified in spectrum c shown in the inset of Figure 1. Spectrum 1c shows the ^{40}Ti proton decay events of setting 2 with the requirement of a β ray in the upstream or downstream β detector with $\Delta E_\beta \leq 650$ keV. In addition, this spectrum contains only decays that occurred within one ^{40}Ti half-life (51.7(6) ms, see below) after the implantation of the corresponding ^{40}Ti atom. This decreased the ^{40}Ti statistics by a factor of two, but reduced the low-energy β background, mainly from ^{38}Ca decay, by a much larger factor.

We identified a total of twenty-one ^{40}Ti proton decay lines; the "line" at 4.353(99) MeV is an unresolved group of transitions. The energies of the proton groups and their absolute decay branching ratios, I_p, obtained by dividing the proton intensities by the number of implanted ^{40}Ti atoms (the latter were corrected for losses from secondary reactions in the stopping process [11]) are shown in Table 1, along with the low-statistics results of Détraz *et al.* [4]. When proton branching ratios were extracted under several β gating conditions the individual intensities of weak lines varied up to 2σ. However, the summed branches were consistent at 1σ level.

The γ ray signal in the germanium detectors was used to distinguish between β-delayed proton decays of ^{40}Ti to the ground (βp_0) and 2.469 MeV first excited state of ^{39}Ca (βp_1). The proton lines at 1.322(9) and 1.957(79) MeV were in coincidence with 2.469 MeV γ rays and identified as βp_1 transitions. The proton line at 1.574 MeV seemed to be coincident with Compton γ rays and was tentatively assigned to a βp_1 transition; β-proton decays of ^{40}Ti to other low-lying states in ^{39}Ca [12] are less probable for spin/parity reasons. Furthermore, $\beta\gamma$-proton decay is unlikely to compete significantly with βp_1 decay since the γ widths of highly unbound states are usually much smaller than their proton widths (the isospin-forbidden proton decay of the ^{40}Sc IAS could be an exception to this general expectation).

No conclusions could be drawn about the origins of the weak proton lines 1 and 2 in Table 1; the statistics of the coincident 2.469 MeV or Compton γ events were consistent with both βp_0 and βp_1 decay modes. Because the excitation energies of the ^{40}Sc 1^+ levels corresponding to the strong proton lines 5 and 7, 2.281(9) and 2.753(11) MeV, are close to the 1^+ ^{40}K states at 2.28988(3) and 2.73038(4) MeV [12], we identify these levels as isospin analogs. No other known or possible ^{40}K 1^+ levels occur in the well-studied region below 2.9 MeV. If lines 1 or 2 were due to βp_0 decays of ^{40}Ti, it would imply the existence of an unknown ^{40}K 1^+ level at low excitation energies or that the ^{40}Sc analog of the ^{40}K level at 2.28988 MeV was shifted downward by at least 0.6 MeV. Both possiblities are very unlikely. We therefore assigned these two lines to βp_1 decays. For all other ^{40}Ti proton lines, βp_1 decay could be excluded by the absence of the corresponding γ events.

The germanium detector spectrum in coincidence with β rays in the implantation detector showed no evidence for ^{40}Ti $\beta\gamma$ decays. From the β-signals in this counter an upper limit of 0.7% for the sum of all possible $\beta\gamma$-branchings could be extracted. Furthermore, no evidence was found for a possible $\beta\gamma$-proton decays of ^{40}Ti via the ^{40}Sc IAS. These isovector γ decays should have the same partial widths as the (bound) mirror IAS in ^{40}K [12] and therefore would feed ^{40}Sc states at 2.281 and 2.753 MeV with the subsequent emission of 1.698 and 2.159 MeV protons. The energies of the ^{40}Sc states and the absolute ^{40}Ti β-decay intensities I_β are shown in Table 2.

The ^{40}Ti half-life was extracted from the time differences between the stopped atoms and their subsequent decay events. A background of β rays or fast charged particles penetrating all three detectors was excluded by a two-dimensional condition on proton energy versus the β-detector signals. Corrections were made for a small background in the time spectrum arising from ^{40}Ti, ^{41}Ti or ^{37}Ca decay events where the arrival of the corresponding atom was missed for dead-time reasons, and for events where a second heavy ion closed the correlation gate *before* the first ion had decayed. The resulting ^{40}Ti half-life of 51.7(6) ms can be compared with the previous value 56^{+18}_{-12} ms [4]. Our ^{41}Ti half-life, 80.1(9) ms, agrees with the previous, less precise, value of 80(2) ms [13].

The β-decay transition strengths were computed using the relation

$$(B(F) + B(GT))_i = \frac{K}{f(E_i)t_i}$$

where $B(F)$ is the Fermi strength, $K = 6127(9)$ s [17], and E_i, t_i and $f(E_i)$ are the β-endpoint energy, the partial half-life and the phase-space factor [18], respectively, of a β transition to state i in ^{40}Sc. The phase space factor is a strong function of the energy release in the decay, the uncertaintly of which is dominated by the $\pm$160 keV uncertainty in the ^{40}Ti mass [14, 16]. We finessed this problem by using the isobaric multiplet mass equation (IMME) to predict the ^{40}Ti mass from the precisely known masses of the other four members of the lowest lying A = 40, T = 2 multiplet. The mass excess of the $T_z = -1$ member, -16160.8(9.2) keV, determined from our measured excitation energy of the IAS in ^{40}Sc, agrees well with the quadratic IMME prediction -16161.2(6.1) keV. From the mass excesses of the $T_z = 2, 1, 0$, and -1 members, -35039.890(4), -29151.0(4), -22858.1(2.0), and -16160.8(9.2) keV [12, 14] respectively, we predict a ^{40}Ti mass excess of -9060(12) keV. Because, as shown in Table 3, the quadratic IMME provides an excellent fit to the well-known multiplet masses ($\chi^2/\nu = 1.19$, $P(\chi^2, \nu) = 0.30$), we conclude that the measured ^{40}Ti mass excess, -8850(160) keV, is off by about 1.3σ, and deduce from the IMME equation an electron capture Q value of 11466(13) keV for ^{40}Ti decay to the ground state of ^{40}Sc. The resulting $B(F) + B(GT)$ values are shown in Table 2.

The observed strength, $B(F) = 3.90(25)$, of the pure Fermi transition to the 4.365(8) MeV IAS agrees well with the model-independent value $B(F) = |Z - N| = 4$, providing an impressive overall check on our absolute β-decay branching ratios. It is possible that part of the Fermi strength is mixed into $J^\pi = 0^+$; $T = 1$ states that may lie close to the IAS [2]. Because we cannot exclude the possibility that the ^{40}Sc state at 4.265(22) MeV is a 0^+, $T = 1$ level fed in a isospin-forbidden Fermi transition carrying 5% of the total Fermi strength, we give this level a $J^\pi = (0, 1)^+$ assignment. The strengths of the transitions to the remaining states indicate allowed transitions and hence 1^+ assignments.

Figure 2 compares our integrated ^{40}Ti GT strength as a function of excitation

energy in ^{40}Sc to the shell-model calculation [2]. The *shape* of the integrated strength is well reproduced by the theory, but the theoretical excitation energies are generally about 0.5-1.0 MeV too high; a similar failure has been been observed in ^{37}Ca decay [19]. Furthermore, the strength is spread over more levels than predicted by the theory, especially around $E_x = 3$ MeV. This is presumably due to higher-order correlations neglected in the model; these can fragment the GT strength without significantly changing its magnitude.

The ICARUS detector is expected to have an electron energy threshold of $W = 5$ MeV for charged-current capture events [1]. The capture cross-section of ^{8}B neutrinos on ^{40}Ar, with this threshold on the outgoing electron, was calculated following the procedure described in Ref. [2] except that the ^{8}B neutrino spectrum of [20] was used. Cross sections were computed using the ^{40}K excitation energies [12] for the IAS and the lowest two 1^+ states (see Table 2). We could not find definitive ^{40}K analogs for the remaining ^{40}Sc daughters fed in ^{40}Ti decay, and were forced to use ^{40}Sc energies in those cases. However, the uncertainty introduced by this approximation is very small as these remaining transitions account for only 21% of the total cross section and the excitation energy shifts are likely to be only some tens of keV. We used the measured B value for the ^{40}Ar capture rate into the IAS in ^{40}K instead of the theoretical value $B(F) = 4$. The actual B value could well be less than 4 (if isospin mixing removed some of the Fermi strength) or exceed 4 (if a Gamow-Teller transition to a 1^+ level were not resolved from the Fermi transition to the IAS). The resulting ^{40}Ar neutrino cross sections for ^{8}B neutrinos, along with the $B(F) + B(GT)$ values used in the computation are shown in Table 2.

The sum of the cross sections is $14.5(4)\times10^{-43}$ cm^2, about 73% of which arises from Gamow-Teller transitions. Ormand *et al.* predicted a cross section of $11.5(7)\times10^{-43}$ cm^2. As can be seen from Figure 2, much of the discrepancy between experiment and theory is due to the failure of the theory to reproduce the excitation energies. Our ^{40}Ar cross section for absorbing ^{8}B neutrinos corresponds to a neutrino capture rate of $9.6^{+1.4}_{-1.7}$ SNU [21].

In summary, we have used the mirror β decay of ^{40}Ti to obtain an empirical

value for the ^{40}Ar cross section for absorbing ^{8}B neutrinos. About 73% of the ^{40}Ar neutrino capture rate arises from Gamow-Teller transitions. This increases the charged-current efficiency of the ICARUS detector over the original prediction which assumed that the cross section was dominated by the Fermi transition. A more detailed discussion of the results will be presented elsewhere [22].

This work was supported by the *Training and Mobility of Researchers* programme of the Commission of the European Communities, under Contract N° ERBFMBICT950394; by US National Science Foundation grants PHY94-02761 and PHY96-00202 and the Warren Foundation at the University of Notre Dame and by a US Department of Energy grant at the University of Washington.

References

[1] ICARUS Collaboration, ICARUS II Proposal (1993), *A second-generation proton decay experiment and neutrino observatory at the Gran Sasso Laboratory.*

[2] W.E. Ormand et al., Phys. Lett. B345 (1995) 343.

[3] J.N. Bahcall et al., Phys. Lett. B178 (1986) 324.

[4] C. Détraz et al., Nucl. Phys. A519 (1990) 529.

[5] R. Anne et al., Nucl. Instr. Meth. A257 (1987) 215.

[6] A.C. Mueller and R. Anne, Nucl. Instr. Meth. B56/57 (1991) 559.

[7] R. Anne and A.C. Mueller, Nucl. Instr. Meth. B70 (1992) 276.

[8] A. Honkanen et al., Nucl. Phys. A, in print.

[9] C. Chasman et al., Phys. Rev. Lett. 15 (1965) 245.

[10] A. Piechaczek et al., Nucl. Phys. A584 (1995) 509.

[11] W. Trinder, Ph.D. thesis, Universität Frankfurt a.M. (1995).

[12] P.M. Endt, Nucl. Phys. A521 (1990) 1.

[13] R.G. Sextro et al., Nucl. Phys. A234 (1974) 130.

[14] G. Audi and A.H. Wapstra, Nucl. Phys. A595 (1995) 409.

[15] M.S. Antony et al., At. Data Nucl. Data Tables 33 (1985) 447.

[16] C.L. Morris et al., Phys. Rev. C25 (1982) 3218.

[17] D.H. Wilkinson, Nucl. Instr. Meth. A335 (1993) 172, 201.

[18] D.H. Wilkinson and B.E.F. Macefield, Nucl. Phys. A232 (1974) 58.

[19] N.I. Kaloskamis et al., Phys. Rev. C55 (1997) 630.

[20] J.N. Bahcall and B.R. Holstein, Phys. Rev. C33 (1986) 2121.

[21] J.N. Bahcall et al., Rev. Mod. Phys. 67 (1995) 781.

[22] M. Bhattacharya et al., to be published.

Table 1: Absolute β-delayed proton intensities in ^{40}Ti decay.

Line	E_p(MeV) this work	I_p	E_p(MeV) ref. [4]	I_p
(1	0.709(25)	0.0034(10))		
2	1.105(26)	0.0031(11)		
3	1.322(9)	0.0346(25)		
4	1.574(28)	0.0045(12)		
5	1.698(9)	0.249(7)	1.84(12)	0.04(2)
6	1.957(79)	0.013(2)		
7	2.159(10)	0.294(14)	2.24(12)	0.20(4)
8	2.355(35)	0.0086(22)		
9	2.481(26)	0.016(3)	2.56(12)	0.03(1)
10	2.708(31)	0.016(3)		
11	2.902(31)	0.013(3)		
12	3.046(23)	0.018(3)		
13	3.153(20)	0.029(4)		
14	3.428(35)	0.011(2)		
15	3.633(21)	0.0099(18)		
16	3.733(12)	0.218(15)	3.84(12)	0.16(4)
17	3.890(33)	0.014(3)		
18	4.015(32)	0.015(4)		
19	4.353(99)	0.02(1)		
20	4.951(60)	0.0063(20)		
21	5.308(33)	0.0068(20)		
TOTAL		1.002(26)		0.43(6)

Table 2: β decays of ^{40}Ti and their isobaric-analog neutrino captures on ^{40}Ar. Excitation energies are given in MeV. The neutrino capture cross sections assume a 5 MeV threshold on the total energy of the outgoing electron; the incoming neutrinos are assumed to have the standard ^{8}B spectrum.

	^{40}Ti decay					^{40}Ar(ν, e)	
i	$E_i(^{40}\mathrm{Sc})$	decay	J^π	I_β	$B(F)+B(GT)$	$E_i(^{40}\mathrm{K})$	$\sigma_\nu(10^{-43}\mathrm{cm}^2)$
1	2.281(9)	p_0	1^+	0.249(7)	0.96(3)	2.290	3.40(10)
2	2.753(11)	p_0	1^+	0.294(14)	1.50(7)	2.730	4.22(21)
3	2.955(35)	p_0	1^+	0.0086(22)	0.050(13)	(3.110)	0.12(3)
4	3.084(26)	p_0	1^+	0.016(3)	0.101(17)		0.23(4)
5	3.317(31)	p_0	1^+	0.016(3)	0.114(20)		0.23(4)
6	3.515(31)	p_0	1^+	0.013(3)	0.105(23)		0.19(4)
7	3.664(23)	p_0	1^+	0.018(3)	0.16(3)		0.26(5)
8	3.758(20)	p_0, p_1	1^+	0.032(5)	0.32(5)		0.49(7)
9	4.055(35)	p_0	1^+	0.011(2)	0.14(3)		0.17(3)
10	4.141(26)	p_1	1^+	0.0031(11)	0.040(14)		0.047(17)
11	4.265(22)	p_0	$(0,1)^+$	0.0099(18)	0.14(3)		0.15(3)
12	4.365(8)	p_0, p_1	0^+	0.252(16)	3.90(25)	4.384	3.87(25)
13	4.528(33)	p_0	1^+	0.014(3)	0.24(6)		0.21(5)
14	4.637(29)	p_0, p_1	1^+	0.020(4)	0.38(8)		0.30(6)
15	5.003(99)	p_0, p_1	1^+	0.056(6)	0.9(3)		0.48(15)
16	5.617(61)	p_0	1^+	0.0063(20)	0.28(9)		0.09(3)
17	5.983(33)	p_0	1^+	0.0068(20)	0.44(13)		0.10(3)

Table 3: Coefficients of the IMME for the lowest $T = 2$ multiplet in $A = 40$.

a (keV)	b (keV)	c (keV)	d (keV)	e (keV)	χ^2/ν	P(χ^2/ν)
−22857.9(1.6)	−6495.2(2.4)	202.1(8)			1.19	0.30
−22858.3(2.5)	−6495.8(4.1)	203.7(6.2)	−0.6(2.3)		2.28	0.13
−22858.1(2.6)	−6495.8(6.0)	203.0(7.7)		−0.1(1.2)	2.36	0.12
−22858.1(2.0)	−6478(15)	194(9)	−17(13)	9(7)		

Figure 1: Delayed proton spectra from ^{40}Ti β decay. Panel a shows the raw spectrum at setting 2 while panel b shows the β-coincident spectrum at setting 1. The inset (spectrum c) is part of the β-coincident spectrum of setting 2, but with the requirement of a short decay-time window (see text). The energy scale refers to the detector signal (decay energy minus recoil loss); the mean shift due to β summing has been subtracted.

Figure 2: Comparison of the integrated $B(GT)$ strength (solid lines indicating the $\pm 1\sigma$ uncertainty band) with a shell-model calculation [2] (dashed line).

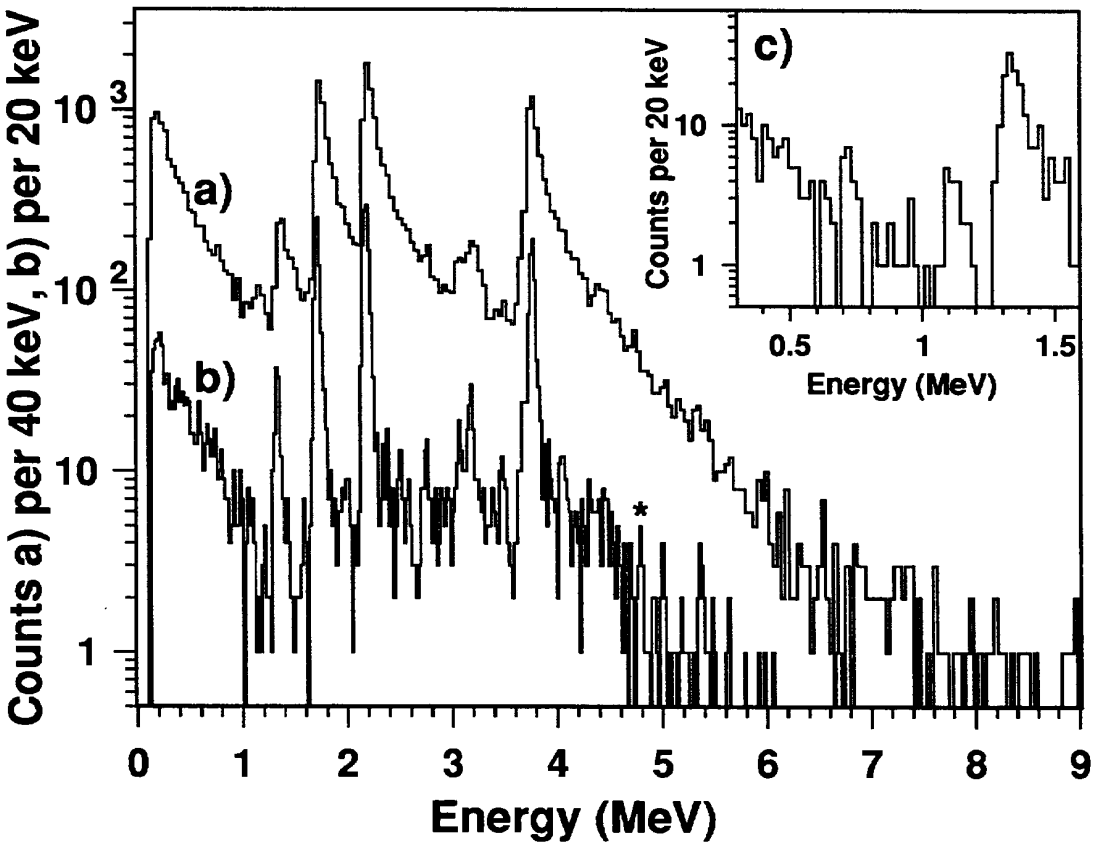
Counts a) per 40 keV, b) per 20 keV
Energy (MeV)
a)
b)
c)
*
Counts per 20 keV
Energy (MeV)

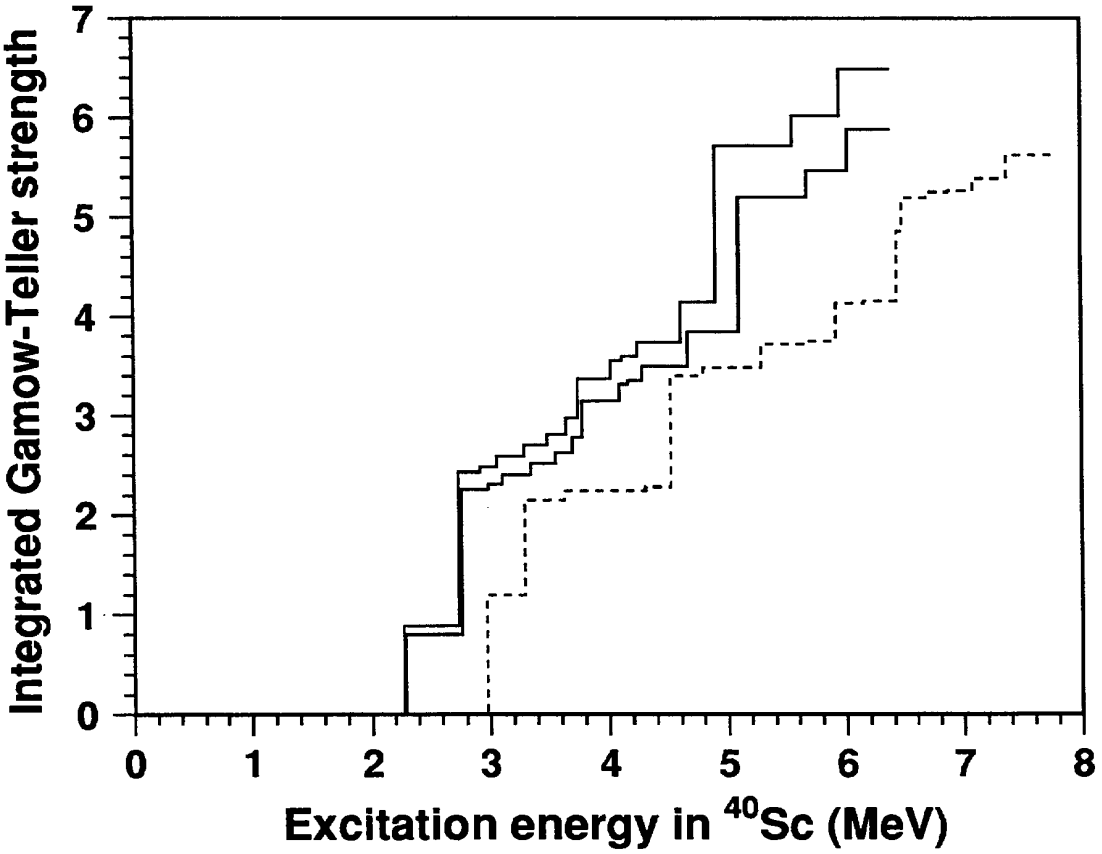
Integrated Gamow-Teller strength
0
1
2
3
4
5
6
7
0
1
2
3
4
5
6
7
8
Excitation energy in ^{40}Sc (MeV)